ELSEVIER

Journal of Computational and Applied Mathematics 97 (1998) 81–97

JOURNAL OF COMPUTATIONAL AND APPLIED MATHEMATICS

Numerical analysis of radially nonsymmetric blow-up solutions of a nonlinear parabolic problem

Stefka Dimova[a,*], Michael Kaschiev[b], Milena Koleva[b], Daniela Vasileva[b]

[a] *Faculty of Mathematics and Informatics, The University of Sofia, 5 James Bautchier Blvd., 1126 Sofia, Bulgaria*

[b] *Institute of Mathematics and Informatics, Bulgarian Academy of Sciences, Bulgaria*

Received 11 July 1997; received in revised form 11 December 1997

Abstract

The process of combustion for a nonlinear heat conducting medium with a nonlinear volume source is considered. Blow-up self-similar solutions which describe the evolution of radially nonsymmetric waves — with complex symmetry and spiral waves — are realized numerically. Their asymptotic behaviour is analysed and their metastability is established. To solve the self-similar nonlinear problem the continuous analog of the Newton method and the finite element method are used. The semidiscrete Galerkin finite element method and an explicit difference scheme are used to solve the nonlinear parabolic problem. Special adaptive grids, consistent with the structure of the self-similar solutions, are utilized.

Keywords: Nonlinear parabolic problem; Blow-up; Self-similar solution; Asymptotic behaviour; Continuous analog of Newton's method; Galerkin finite element method; Adaptive grids

1. Introduction

The blow-up problem is of a great importance when considering nonlinear evolution processes. Blow-up means an explosive instability of the process, when the magnitude of some quantity (e.g. temperature, pressure, density, etc.) tends to infinity in a finite time. The state of evolution of such explosive instabilities has important applications in plasma physics, chemical reactor theory, combustion theory, quantum and fluid mechanics, ecology, technology. Blow-up phenomena are observed in more than 60 different types of problems [22].

From a mathematical point of view the problem of blow-up reduces to the study of solutions of nonlinear evolution equations that become unbounded (blow-up) in a finite time. A general theory of such strongly nonlinear phenomena does not yet exist. During the last 20–25 years there has been an explosion of interest in blow-up theorems (see the review article of Levine [17], the book

* Corresponding author. E-mail: nummeth@math.acad.bg.

0377-0427/98/$19.00
PII S0377-0427(98)00103-4

of Beberness and Eberly [3] and the references cited therein). But most of them were devoted only to semilinear equations (linear diffusion) or systems of such equations with single-point, blow-up solutions.

The blow-up of solutions of quasilinear parabolic equations (nonlinear diffusion) is considered in the book of Samarskii et al. [19]. Besides some important applications to nuclear fusion and confinement, laser thermonuclear synthesis, etc. [16, 20, 23, 24] the investigation of the quasilinear case poses problems that are interesting from another point of view. The combination of nonlinear diffusion with nonlinear volume sources in the medium makes it possible that highly nonstationary dissipative structures and waves arise and evolve into this medium. One of the most important problems of the synergetics is to find all possible classes of structures and waves which may arise and preserve themselves in a given nonlinear medium.

In this paper we will emphasize the synergetic point of view when considering the processes of heat transfer and combustion of a nonlinear medium, described by the equation

$$u_t = \nabla(u^\sigma \nabla u) + u^\beta, \quad t>0,\ x=(x_1,x_2,\ldots,x_N). \tag{1}$$

Here $u(t,x) \geqslant 0$ is the temperature, $\sigma>0$ and $\beta>1$ are medium parameters. The heat conductivity coefficient $k(u)=u^\sigma$ and the self-generating volume source $q(u)=u^\beta$ are power functions of the temperature. Not only is this choice reasonable for many applications, but it also makes Eq. (1) possess a number of different invariant solutions [11]. As a consequence, it makes the medium rich of different classes of structures and waves. Simple radially symmetric structures (monotone in r with one maximum at the origin) for $\beta \geqslant \sigma+1$ and complex ones (nonmonotone in r) for $\beta>\sigma+1$ were found and investigated in many works (see [7, 9–11, 19] and the references cited therein). Two classes of structures with *complex symmetry* (i.e., different from radial symmetry) were found and analysed in the essentially two-dimensional case when $\beta>\sigma+1$ [1, 13, 15]. For $\beta<\sigma+1$ only simple radially symmetric waves were found. The main contributions of this work are the numerical realization and analysis of two classes of radially nonsymmetric waves in a two-dimensional nonlinear medium, described by Eq. (1) in polar coordinates (r,φ) with $\beta<\sigma+1$. These radially nonsymmetric waves are invariant (in particular, self-similar) blow-up solutions of the corresponding nonlinear equation, like all of the structures mentioned above.

For $N=2$ Eq. (1) in polar coordinates reads:

$$u_t = \frac{1}{r}\frac{\partial}{\partial r}\left(ru^\sigma \frac{\partial u}{\partial r}\right) + \frac{1}{r^2}\frac{\partial}{\partial \varphi}\left(u^\sigma \frac{\partial u}{\partial \varphi}\right) + u^\beta, \quad t>0,\ 0<r<\infty,\ 0 \leqslant \varphi < 2\pi. \tag{2}$$

By using the method of invariant-group analysis it was shown in the Ph.D. Thesis of S.R. Svirshchevskii (1985) that Eq. (2) admits blow-up self-similar solutions of the kind [2]:

$$u(t,r,\varphi) = g(t)\theta(\xi,\phi), \qquad g(t) = (1-t/T_0)^{-1/(\beta-1)}, \tag{3}$$

$$\xi = r/\psi_1(t) = r(1-t/T_0)^{-m}, \qquad m = \frac{\beta-\sigma-1}{2(\beta-1)}, \tag{4}$$

$$\phi = \varphi + \psi_2(t) = \varphi + \frac{C_0}{\beta-1}\ln(1-t/T_0). \tag{5}$$

Here $T_0>0$ is the blow-up time, C_0 is a parameter of the family of solutions. The function $\theta(\xi,\phi)\geqslant 0$ satisfies the nonlinear elliptic equation

$$-\frac{1}{\xi}\frac{\partial}{\partial\xi}\left(\xi\theta^{\sigma}\frac{\partial\theta}{\partial\xi}\right)-\frac{1}{\xi^2}\frac{\partial}{\partial\phi}\left(\theta^{\sigma}\frac{\partial\theta}{\partial\phi}\right)+\frac{\beta-\sigma-1}{2(\beta-1)T_0}\xi\frac{\partial\theta}{\partial\xi}-\frac{C_0}{(\beta-1)T_0}\frac{\partial\theta}{\partial\phi}$$
$$+\frac{1}{(\beta-1)T_0}\theta-\theta^{\beta}=0,\quad 0<\xi<\infty,\ 0\leqslant\phi<2\pi. \tag{6}$$

As a function of the new, similarity variables ξ,ϕ, where the time t and the space (r,φ) are connected in a special way, given by (4), (5), $\theta(\xi,\phi)$ defines the space–time structure of the self-similar solution (3). As a nonlinear equation, (6) may have multiple solutions. Thus, the different solutions of (6) will determine a set of possible structures ($\beta\geqslant\sigma+1$) and waves ($\beta<\sigma+1$) in the corresponding medium. That is why the solutions of (6) are called *eigenfunctions* of combustion of this medium [14].

Let us note, that it is not possible to realize numerically complex self-similar solution of the type (3)–(5), taking arbitrary initial data when solving Eq. (2). So a very important problem is to find all the different solutions of the self-similar Eq. (6). Taking them as initial data for Eq. (2), we would find the corresponding structures and waves in the medium.

Eq. (6) has two homogeneous solutions: $\theta_{\mathrm{H}}^0\equiv 0$ and $\theta_{\mathrm{H}}^1\equiv[(\beta-1)T_0]^{-1/(\beta-1)}$. For convenience and, without loss of generality, we set $T_0=(\beta-1)^{-1}$ in (6):

$$\mathscr{L}(\theta)\equiv-\frac{1}{\xi}\frac{\partial}{\partial\xi}\left(\xi\theta^{\sigma}\frac{\partial\theta}{\partial\xi}\right)-\frac{1}{\xi^2}\frac{\partial}{\partial\phi}\left(\theta^{\sigma}\frac{\partial\theta}{\partial\phi}\right)+\frac{\beta-\sigma-1}{2}\xi\frac{\partial\theta}{\partial\xi}-C_0\frac{\partial\theta}{\partial\phi}$$
$$+\theta-\theta^{\beta}=0,\quad 0<\xi<\infty,\ 0\leqslant\phi<2\pi. \tag{7}$$

Then $\theta_{\mathrm{H}}^1\equiv 1$.

The case $C_0=0$ is analysed in [1, 13, 15]. Radially nonsymmetric eigenfunctions of complex symmetry, satisfying the following boundary conditions:

$$\lim_{\xi\to 0}\xi\theta^{\sigma}\frac{\partial\theta}{\partial\xi}=0,\qquad \frac{\partial\theta}{\partial\phi}=0\quad\text{for }\phi=0\text{ and }\phi=2\pi, \tag{8}$$

$$\lim_{\xi\to\infty}\theta(\xi,\phi)=\theta_{\mathrm{H}}^0\equiv 0, \tag{9}$$

are found numerically when $\beta>\sigma+1$. For $\beta\leqslant\sigma+1$ with the same boundary conditions only simple radially symmetric eigenfunctions are found in the above cited works. To find radially nonsymmetric eigenfunctions when $\beta<\sigma+1$ we pose another boundary condition instead of (9):

$$\lim_{\xi\to\infty}\theta(\xi,\phi)=\theta_{\mathrm{H}}^1\equiv 1, \tag{10}$$

i.e., we seek for solutions of (7), which tend to the second homogeneous solution $\theta_{\mathrm{H}}^1\equiv 1$ at infinity. For the solutions of (2) this means that $u(t,r,\varphi)$ is bounded at infinity for every fixed t, $0\leqslant t<T_0$.

The case $C_0\neq 0$ is considered in [8], where good approximations to the eigenfunctions for $\beta<\sigma+1$ are found and analysed. The computation of the eigenfunctions was announced in [5, 6]. Here we describe the numerical method and analyse the asymptotic behaviour of the self-similar solution (3)–(5) for $\beta<\sigma+1$.

The paper is organized as follows. In Section 2 we discuss some properties of the self-similar solution (3)–(5). Definitions of structural stability and metastability of these blow-up solutions and, therefore, of the corresponding dissipative structures and waves, are given. In Sections 3 the construction of approximations to the eigenfunctions $\theta(\xi,\phi)$ is described. On the basis of their asymptotic behaviour a boundary condition of third kind for the self-similar elliptic problem is derived. Sections 4 and 5 are devoted to the numerical methods used for solving the self-similar elliptic problem and the parabolic problem respectively. In Section 6 the results of some numerical experiments are given. The evolution in time of five different eigenfunctions, corresponding to the same parameters σ and β is shown and their stability is analysed. The reliability and accuracy of both numerical methods are discussed.

2. Preliminaries

Let us consider the self-similar blow-up solution (3)–(5). As mentioned in [2], if the temperature profile has inhomogeneities (for example local maxima) at the initial time then their trajectories will be logarithmic spirals. Denoting by $(r(t),\varphi(t))$ the coordinates of such an inhomogeneity at time t, one gets

$$\begin{aligned} &r(t)e^{s\varphi(t)} = r(0)e^{s\varphi(0)} = \xi e^{s\phi}, \qquad s = \frac{\beta-\sigma-1}{2C_0}, \\ &\frac{1}{s}\ln r(t) + \varphi(t) = \frac{1}{s}\ln\xi + \phi = \text{const}. \end{aligned} \tag{11}$$

It is clear that the propagation direction for fixed C_0 depends on the relation between σ and β: for $\beta<\sigma+1$ (the so-called *HS-evolution*) the inhomogeneities move from the centre along the spiral; for $\beta>\sigma+1$ they move towards the center (LS-*evolution*). At $\beta=\sigma+1$ (*S-evolution*) the spirals degenerate into circles.

In order to define two kinds of stability of the self-similar solution (3)–(5), we will introduce the self-similar representation $\Theta(t,\xi,\phi)$ of the solution $u(t,r,\varphi)$ of Eq. (2), corresponding to the initial data $u_0(r,\varphi)$:

$$\begin{aligned} &\Theta(t,\xi,\phi) = u(t,r,\varphi)/\Gamma(t), \qquad \xi = r\Gamma(t)^{(\beta-\sigma-1)/2}, \qquad \phi = \varphi - C_0\ln(\Gamma(t)), \\ &\Gamma(t) = \max_{\bar\Omega} u(t,r,\varphi)/\max_{\bar\Omega} u_0(r,\varphi), \qquad \bar\Omega = [0,\infty)\times[0,2\pi). \end{aligned} \tag{12}$$

The self-similar solution, corresponding to the eigenfunction $\theta(\xi,\phi)$ is called *structurally stable* [19], if there exists a class of initial data $u_0(r,\varphi)\neq\theta(r,\varphi)$, so that for the self-similar representations $\Theta(t,\xi,\phi)$ of the corresponding solutions $u(t,r,\varphi)$:

$$\|\Theta(t,\cdot,\cdot) - \theta(\cdot,\cdot)\|_{C(\bar\Omega)} \to 0, \quad t\to T_0^-, \tag{13}$$

where the uniform norm in $\bar\Omega$ is denoted by $\|\cdot\|_{C(\bar\Omega)}$.

A natural question arises: *if we take some eigenfunction $\theta(\xi,\phi)$ as initial data for Eq. (2), will the corresponding self-similar solution always be structurally stable?* The answer is "no". All numerical investigations, carried out in the radially symmetric case [7, 9–11] as well as in the essentially two-dimensional case [1, 13, 15], show that (13) is fulfilled only for the simplest, radially

symmetric and radially decreasing eigenfunction $\theta(\xi,\phi)=\theta(\xi)$. Theoretical investigations have been carried out only in the one-dimensional case [11, 19].

Then a second question arises: *why are the self-similar solutions considered, if most of them are not structurally stable?* The answer is – they could be *metastable* in the following sense. For every $\varepsilon>0$ there exists a class of initial data $u_0(r,\varphi)\approx\theta(r,\varphi)$ and a time T, $T_0-T\ll T_0$, such that for the self-similar representations of the corresponding solutions

$$\|\Theta(t,\cdot,\cdot)-\theta(\cdot,\cdot)\|_{C(\bar{\Omega})}\leqslant\varepsilon \quad \text{for } 0\leqslant t\leqslant T. \tag{14}$$

This means the self-similar solutions preserve their structure up to time T, very close to the blow-up time T_0. For $t\geqslant T$ the complex structure, corresponding to the complex eigenfunction, degenerates into one or more simple structures, described by the simplest eigenfunction for the same parameters σ,β.

3. Approximations to the eigenfunctions

It is proved in [19] that when $\beta<\sigma+1$ there exists an infinite number of radially symmetric solutions of (7), which tend to θ_H^1 when $\xi\to\infty$. This allows us to suppose the existence of eigenfunctions with an analogous behaviour in the essentially two-dimensional case. Using the assumption for small oscillations of the eigenfunctions about the homogeneous background $\theta_H^1\equiv 1$, i.e.,

$$\theta(\xi,\phi)=1+\alpha y(\xi,\phi), \quad |\alpha y|\ll 1$$

and the idea of linearization around it [1, 7, 9–11, 13, 15, 19], the following linear equation for $y(\xi,\phi)$ is found [8]:

$$-\frac{1}{\xi}\frac{\partial}{\partial\xi}\left(\xi\frac{\partial y}{\partial\xi}\right)-\frac{1}{\xi^2}\frac{\partial^2 y}{\partial\phi^2}+\frac{\beta-\sigma-1}{2}\xi\frac{\partial y}{\partial\xi}-C_0\frac{\partial y}{\partial\phi}+(1-\beta)y=0. \tag{15}$$

Looking for particular solutions of the kind

$$Y_k(\xi,\phi)=R_k(\xi)e^{ik\phi}, \quad k\in\mathbb{N}$$

which are bounded at $\xi=0$, it is found in [8] that for $\beta\neq\sigma+1$

$$R_k(\xi)=\xi^k\ {}_1F_1(a,b,z).$$

Here ${}_1F_1(a,b,z)$ is the confluent hypergeometric function,

$$a=-\frac{\beta-1+ikC_0}{\beta-\sigma-1}+\frac{k}{2}, \qquad b=1+k, \qquad z=\frac{\beta-\sigma-1}{4}\xi^2.$$

It is shown in [8] that

$$y_k(\xi,\phi)=\mathrm{Re}(Y_k(\xi,\phi))$$

is a solution of (15) as well and it suffices to examine only the case $k>0$, $C_0>0$. When $C_0>0$ the functions $y_k(\xi,\phi)$ are periodic of period $2\pi/k$. When $C_0=0$, they have k-axis of symmetry. Using the asymptotic expansion of ${}_1F_1(a,b,z)$ for $|z|\to\infty$ it is shown [8]:

if $\beta<\sigma+1$, then $|R_k(\xi)|\to 0$, $\xi\to\infty$.

More detailed analysis gives:

$$y_k(\xi,\phi) \sim c\xi^{1/m} \cos k\left(\phi + \frac{1}{s}\ln\xi\right), \quad \xi \to \infty, \tag{16}$$

c is a constant, depending on k, σ, β, and C_0. The asymptotic expression (16) predicts the following asymptotic form for $\theta(\xi,\phi) = \theta_k(\xi,\phi)$, $k = 1,2,\ldots$:

$$\theta_k(\xi,\phi) \sim 1 + \gamma\xi^{1/m} \cos k\left(\phi + \frac{1}{s}\ln\xi\right), \quad \xi \to \infty, \ \gamma = \alpha c \tag{17}$$

which yields the approximation:

$$\tilde{\theta}_k(\xi,\phi) = 1 + \alpha y_k(\xi,\phi), \quad \alpha = \text{const.} \tag{18}$$

When $C_0 = 0$ we choose the value of α so that the condition $\tilde{\theta}_k(\xi,\phi) > 0$ is fulfilled. For $C_0 > 0$ we choose the value of α small enough – the analysis of the evolution in time of the approximations (18) showed [8] that for small α they are close to the eigenfunctions.

From (17) we derive a boundary condition of third kind at $\xi = l \gg 1$:

$$\begin{aligned} \frac{\partial\theta_k}{\partial\xi} &= \frac{\theta_k - 1}{m\xi} - \frac{\gamma k}{s\xi^{(m-1)/m}} \sin k\left(\phi + \frac{1}{s}\ln\xi\right), \quad C_0 \neq 0, \\ \frac{\partial\theta_k}{\partial\xi} &= \frac{\theta_k - 1}{m\xi}, \quad C_0 = 0. \end{aligned} \tag{19}$$

4. Numerical method for the self-similar problem

To solve numerically the problem (7),(8),(19), we use the continuous analog of the Newton method (CANM) [12]. When applied to the nonlinear equation (7) $\mathscr{L}(\theta) = 0$, the CANM leads to the iteration process

$$\mathscr{L}'(\theta_n)v_n = -\mathscr{L}(\theta_n), \tag{20}$$

$$\theta_{n+1} = \theta_n + \tau_n v_n, \quad 0 < \tau_n \leqslant 1, \ n = 0,1,\ldots, \tag{21}$$

$$\theta_0 = \tilde{\theta}_k(\xi,\phi). \tag{22}$$

Here $\mathscr{L}'(\theta_n)$ is the Frechét derivative of the operator $\mathscr{L}$ at the point θ_n, θ_0 is the initial approximation (18) to one of the sought after different eigenfunctions $\theta_k(\xi,\phi)$ for given parameters σ, β. For convenience the subscript k is omitted in (20),(21) and below. As $\tilde{\theta}_k(\xi,\phi)$, $k = 1,2,\ldots$ satisfy the boundary conditions (8),(19), the iteration corrections v_n, $n = 0,1,\ldots$ must satisfy

$$\lim_{\xi\to 0} \xi\theta_n^{\sigma}\frac{\partial v_n}{\partial\xi} = 0, \tag{23}$$

$$\frac{\partial v_n}{\partial\xi} = \frac{v_n}{m\xi} - \left\{\frac{\partial\theta_n}{\partial\xi} - \frac{\theta_n - 1}{m\xi} + \frac{\gamma k}{s\xi^{(m-1)/m}} \sin k\left(\phi + \frac{1}{s}\ln\xi\right)\right\}, \quad \xi = l \gg 1. \tag{24}$$

Taking into account the symmetry ($C_0=0$) or the periodicity ($C_0>0$) of the functions $\tilde{\theta}_k(\xi,\phi)$, the following symmetry conditions:

$$\frac{\partial v_n}{\partial \phi}(\xi,0)=\frac{\partial v_n}{\partial \phi}\left(\xi,\frac{\pi}{k}\right)=0, \quad 0\leqslant \xi \leqslant l \tag{25}$$

or periodic conditions

$$v_n(\xi,0)=v_n\left(\xi,\frac{2\pi}{k}\right), \qquad \frac{\partial v_n}{\partial \phi}(\xi,0)=\frac{\partial v_n}{\partial \phi}\left(\xi,\frac{2\pi}{k}\right)=0, \quad 0\leqslant \xi \leqslant l \tag{26}$$

must be fulfilled.

The Eq. (20) is linear with respect to the iteration corrections v_n. To solve it, we use the Galerkin finite element method [21]. The weak form of the problem (20),(23)–(25) or (26) is:

For given function $\theta_n \in D$ find $v_n \in H^1$, which satisfies the conditions (23)–(25) or (26) and the integral identity

$$(\mathscr{L}'(\theta_n)v_n, w) = -(\mathscr{L}(\theta_n), w) \quad \text{for } \forall w \in H^1, \tag{27}$$

where

$$D=\left\{\theta(\xi,\phi)\colon \xi^{1/2}\theta, \xi^{1/2}\frac{\partial \theta^{\sigma+1}}{\partial \xi}, \xi^{-1/2}\frac{\partial \theta^{\sigma+1}}{\partial \phi} \in L_2(\Omega)\right\},$$

$$H^1=\left\{w(\xi,\phi)\colon \xi^{1/2}w, \xi^{1/2}\frac{\partial w}{\partial \xi}, \xi^{-1/2}\frac{\partial w}{\partial \phi} \in L_2(\Omega), w(\xi,0)=w\left(\xi,\frac{2\pi}{k}\right) \text{ for } C_0>0\right\},$$

$$\Omega=(0,l)\times(0,\omega), \qquad \omega=\frac{\pi}{k} \quad \text{for } C_0=0, \qquad \omega=\frac{2\pi}{k} \quad \text{for } C_0>0.$$

The left- and the right-hand sides of (27) are:

$$\begin{aligned}(\mathscr{L}'(\theta_n)v_n, w) = \int_\Omega \Bigg\{ & \xi\theta_n^\sigma \frac{\partial w}{\partial \xi}\frac{\partial v_n}{\partial \xi} + \sigma\xi\theta_n^{\sigma-1}\frac{\partial \theta_n}{\partial \xi}\frac{\partial w}{\partial \xi}v_n + \frac{\sigma}{\xi}\theta^{\sigma-1}\frac{\partial \theta_n}{\partial \phi}\frac{\partial w}{\partial \phi}v_n \\ & + \frac{\theta_n^\sigma}{\xi}\frac{\partial w}{\partial \phi}\frac{\partial v_n}{\partial \phi} + \frac{\beta-\sigma-1}{2}\xi^2 w\frac{\partial v_n}{\partial \xi} - \xi C_0 w\frac{\partial v_n}{\partial \phi} \\ & + \xi(1-\beta\theta^{\beta-1})wv_n\Bigg\}\,\mathrm{d}\xi\,\mathrm{d}\phi - \int_0^\omega \xi\sigma\theta_n^{\sigma-1}\frac{\partial \theta_n}{\partial \xi}wv_n\,\mathrm{d}\phi \\ & - \int_0^\omega \frac{\theta_n^\sigma}{m}wv_n\,\mathrm{d}\phi + \int_0^\omega \xi\theta_n^\sigma\frac{\partial \theta_n}{\partial \xi}w\,\mathrm{d}\phi - \int_0^\omega \frac{\theta_n^\sigma}{m}(\theta_n-1)w\,\mathrm{d}\phi \\ & + \int_0^\omega \frac{\gamma k}{s}\xi^{1/m}\theta_n^\sigma \sin k\left(\phi+\frac{1}{s}\ln\xi\right)w\,\mathrm{d}\phi,\end{aligned}$$

$$\begin{aligned}(\mathscr{L}(\theta_n), w) = \int_\Omega \Bigg\{ & \xi\theta_n^\sigma\frac{\partial w}{\partial \xi}\frac{\partial \theta_n}{\partial \xi} + \frac{\theta^\sigma}{\xi}\frac{\partial w}{\partial \phi}\frac{\partial \theta_n}{\partial \phi} + \frac{\beta-\sigma-1}{2}\xi^2 w\frac{\partial \theta_n}{\partial \xi} - \xi C_0 w\frac{\partial \theta_n}{\partial \phi} \\ & + \xi(1-\theta^{\beta-1})w\theta_n\Bigg\}\,\mathrm{d}\xi\,\mathrm{d}\phi - \int_0^{2\pi} \xi\theta_n^\sigma\frac{\partial \theta_n}{\partial \xi}w\,\mathrm{d}\phi\end{aligned}$$

The discretization of (27) by using bilinear finite elements gives a linear algebraic system of equations $AV=B$ at every step of the iteration process (20)–(22). The matrix A is nonsymmetric. To solve the system we use the LU decomposition of A.

The iteration parameter $0<\tau_n \leqslant 1$ is determined in the calculations by the formula

$$\tau_n = \begin{cases} \min(1, \tau_{n-1}\delta_{n-1}/\delta_n) & \text{if } \delta_n \leqslant \delta_{n-1}, \\ \max(\tau_0, \tau_{n-1}\delta_{n-1}/\delta_n) & \text{if } \delta_n > \delta_{n-1} \end{cases}$$

Here δ_n is the uniform norm of $\mathscr{L}(\theta_n)$. When $\delta_n \to 0$, then $\tau_n \to 1$ and the iteration process (20)–(22) reduces to the classical Newton method.

The stop criterion for the iteration process (20)–(22) is $\delta_n < \delta$. In the examples, given below, we have used $\delta = 10^{-6}$ and the number of iterations has been between 8 and 15.

5. Numerical method for the parabolic problem

We solve numerically the following initial boundary-value problem:

$$u_t = \frac{1}{r}(ru^\sigma u_r)_r + \frac{1}{r^2}(u^\sigma u_\varphi)_\varphi + u^\beta, \quad 0<t<\tilde{T}_0, \quad (r,\varphi)\in\Omega, \tag{28}$$

$$\Omega = (0,R)\times(0,\omega),$$

$$ru^\sigma u_r(t,0,\varphi) = 0, \quad t\in[0,\tilde{T}_0), \quad \varphi\in[0,\omega], \tag{29}$$

$$u^\sigma u_r(t,R,\varphi) = 0, \quad t\in[0,\tilde{T}_0), \quad \varphi\in[0,\omega], \tag{30}$$

$$u(0,r,\varphi) = u_0(r,\varphi) = \theta_k(r,\varphi) \geqslant 0, \quad (r,\varphi)\in\bar{\Omega}, \tag{31}$$

— in the case $C_0 = 0$ we have $\omega = \pi/k$ and the following symmetry conditions:

$$u^\sigma(t,r,0)u_\varphi(t,r,0) = u^\sigma(t,r,\omega)u_\varphi(t,r,\omega) = 0, \quad t\in[0,\tilde{T}_0), \quad r\in[0,R], \tag{32}$$

$$u_0(0,\varphi) = \text{const}, \quad u_0(r,\varphi) = u_0(r,2\omega-\varphi); \tag{33}$$

— in the case $C_0 > 0$ we have $\omega = 2\pi/k$ and the following periodic conditions:

$$\begin{aligned} &u(t,r,0) = u(t,r,\omega), \\ &u^\sigma(t,r,0)u_\varphi(t,r,0) = u^\sigma(t,r,\omega)u_\varphi(t,r,\omega), \quad t\in[0,\tilde{T}_0), \quad r\in[0,R], \end{aligned} \tag{34}$$

$$u_0(0,\varphi) = \text{const}, \quad u_0(r,\varphi) = u_0(r,\omega+\varphi), \quad (r,\varphi)\in\bar{\Omega}. \tag{35}$$

The length $R = R(t)$ is chosen so as to avoid the influence of the boundary condition (30) on the numerical solution.

The method for solving (28)–(31), (34), (35) is described in detail in [8]. Here we will note only the main steps.

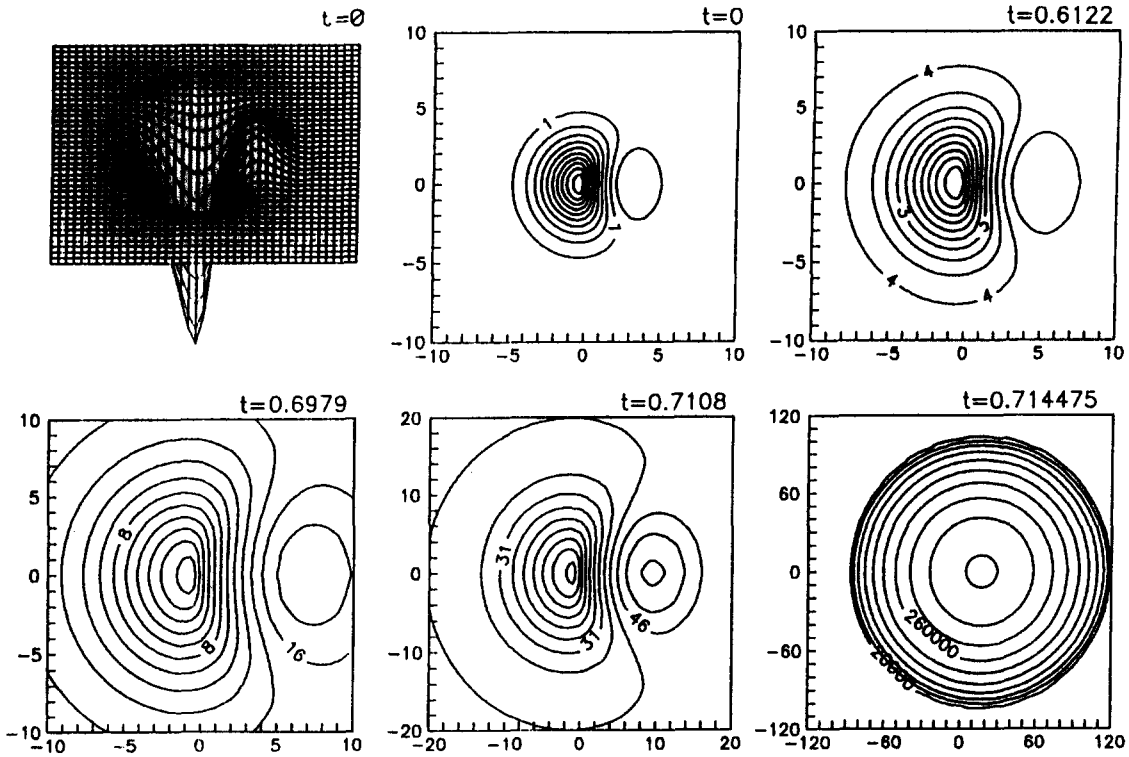

Fig. 1. Evolution of a complex symmetry wave: $C_0 = 0$, $k = 1$.

1. We linearize the elliptic part of the differential operator in (28) by using the Kirchoff transformation:

$$g(u) = \int_0^u w^\sigma \, \mathrm{d}w = \frac{u^{\sigma+1}}{\sigma+1};$$

2. The weak form of the problems (28)–(33) or (28)–(31), (34), (35) is:
Find $u(t, r, \varphi) \in C(0, T_0) \times D$, which satisfies the conditions (29)–(32) or (29)–(31), (34) and

$$(u_t, w) + A(t; u, w) = (f, w) \quad \text{for } \forall w \in H^1, \ 0 < t < \tilde{T}_0,$$

$$u(0, \cdot, \cdot) = u_0,$$

where

$$(u, w) = \int_\Omega ruw \, \mathrm{d}\Omega, \quad f(u) = u^\beta,$$

$$A(t; u, w) = \int_\Omega r \frac{\partial g(u)}{\partial r} \frac{\partial w}{\partial r} + \frac{1}{r} \frac{\partial g(u)}{\partial \varphi} \frac{\partial w}{\partial \varphi} \, \mathrm{d}\Omega;$$

3. We use the lumped mass finite element method [21] in space with interpolation of the nonlinear coefficients [4]. The bilinear basis functions are modified so as to deal successfully with the singularity at the origin and with the periodic boundary conditions for $C_0 > 0$.

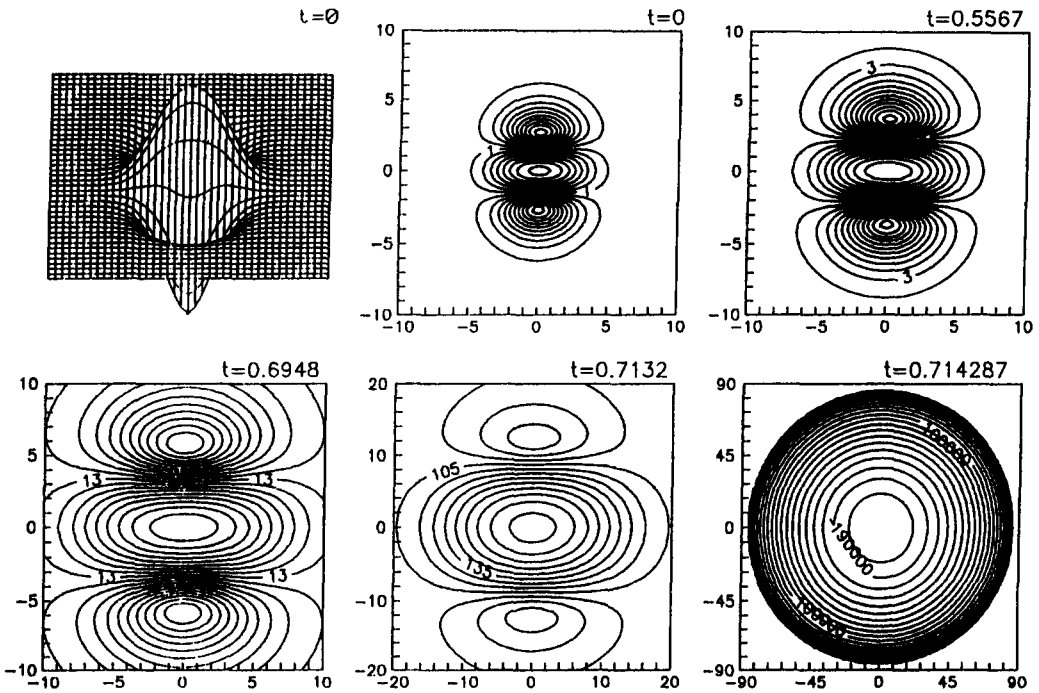

Fig. 2. Evolution of a complex symmetry wave: $C_0 = 0$, $k = 2$.

4. The resulting system of ODE is

$$\dot{\mathbf{U}} = \tilde{\mathbf{M}}^{-1}\mathbf{K}\mathbf{g}(\mathbf{U}) + \mathbf{f}(\mathbf{U}), \tag{36}$$

$$\mathbf{U}(\mathbf{0}) = \mathbf{U}_0. \tag{37}$$

Here $\mathbf{U} = \mathbf{U}(\mathbf{t})$ is the vector, whose components $u_i(t)$ are the values of the numerical solution at the mesh points (r_i, φ_i), $i = 1, \ldots, n$, $\tilde{\mathbf{M}}$ is the lumped mass matrix, $\mathbf{K}$ is the stiffness matrix. Both matrices $\tilde{\mathbf{M}}$ and $\mathbf{K}$ do not depend on the solution u. System (36), (37) is solved by a modification of the Runge–Kutta method [18] which has second order of accuracy and an extended region of stability. The time step τ is chosen automatically so as to guarantee relative stability and a desired accuracy ε at the end of the time interval $[0, \tilde{T}_0)$. The stop criterion is $\tau < 10^{-16}$ and $\tilde{T}_0$ is the time reached in the calculations.

5. A special adaptive grid, consistent with the structure of the self-similar blow-up solution (3)–(5), is used. The step-size in r is chosen so that the step-size in the similarity variable ξ

$$\Delta\xi = \Delta r \left[\frac{\max\limits_{\Omega} u(0, r, \varphi)}{\max\limits_{\Omega} u(t, r, \varphi)} \right]^{(\sigma+1-\beta)/[2(\beta-1)]}$$

is bounded from below. Typically, we satisfy $\Delta\xi \geqslant h_0/2$, where h_0 is the initial step-size in r. This adaptive grid keeps the same number of mesh points in r when increasing $R(t)$ (see Figs. 1–5) and ensures a good accuracy of the numerical solution.

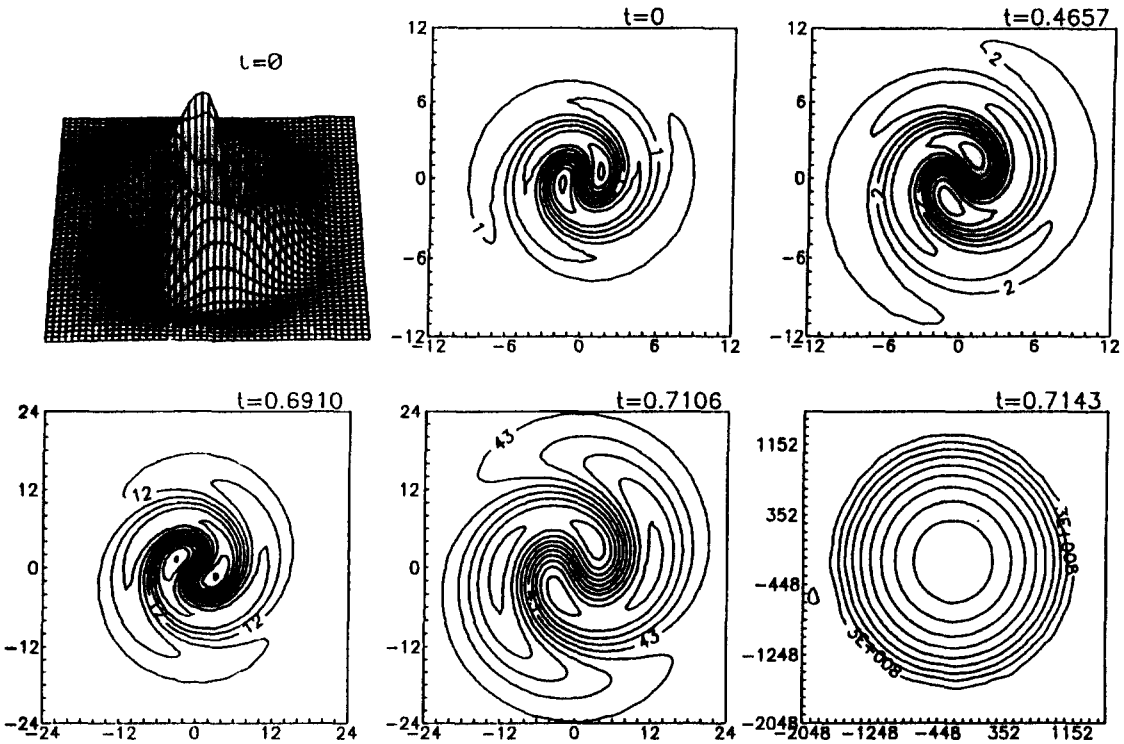

Fig. 3. Evolution of a one-armed spiral wave: $C_0 = 1$, $k = 1$.

6. Numerical experiments

The main goal of the numerical experiments presented here is to analyse the asymptotic behaviour of the radially nonsymmetric blow-up waves with complex symmetry for $C_0 = 0$ and the spiral blow-up waves for $C_0 > 0$ in the medium with parameters $\beta < \sigma + 1$. Simultaneously, the reliability and accuracy of both methods — for solving the nonlinear elliptic and parabolic problems — will be demonstrated.

All our experiments show that the two kinds of waves are metastable. To establish this fact we take the computed eigenfunction $\theta_k(\xi, \phi)$ as initial data for the parabolic problem. We check if the maxima of the eigenfunction follow the self-similar law (11) and compare the self-similar representation $\Theta(t, \xi, \phi)$ given in (12) of the solution $u(t, r, \varphi)$ with the eigenfunction, i.e., we check if (14) is fulfilled for some ε. For this reason we introduce the rescaled error $e(t)$:

$$e(t) = \frac{\max\limits_{i=1}^{n} |\Theta(t, r_i, \varphi_i) - \theta(r_i, \varphi_i)|}{\max\limits_{i=1}^{n} \theta(r_i, \varphi_i) - \min\limits_{i=1}^{n} \theta(r_i, \varphi_i)}. \tag{38}$$

We give these errors for different times t in the first two examples below.

A good criterion for the accuracy of the methods for solving both the elliptic and the parabolic problems is the restoration of the blow-up time. Since we have put $T_0 = 1/(\beta - 1)$ in the elliptic

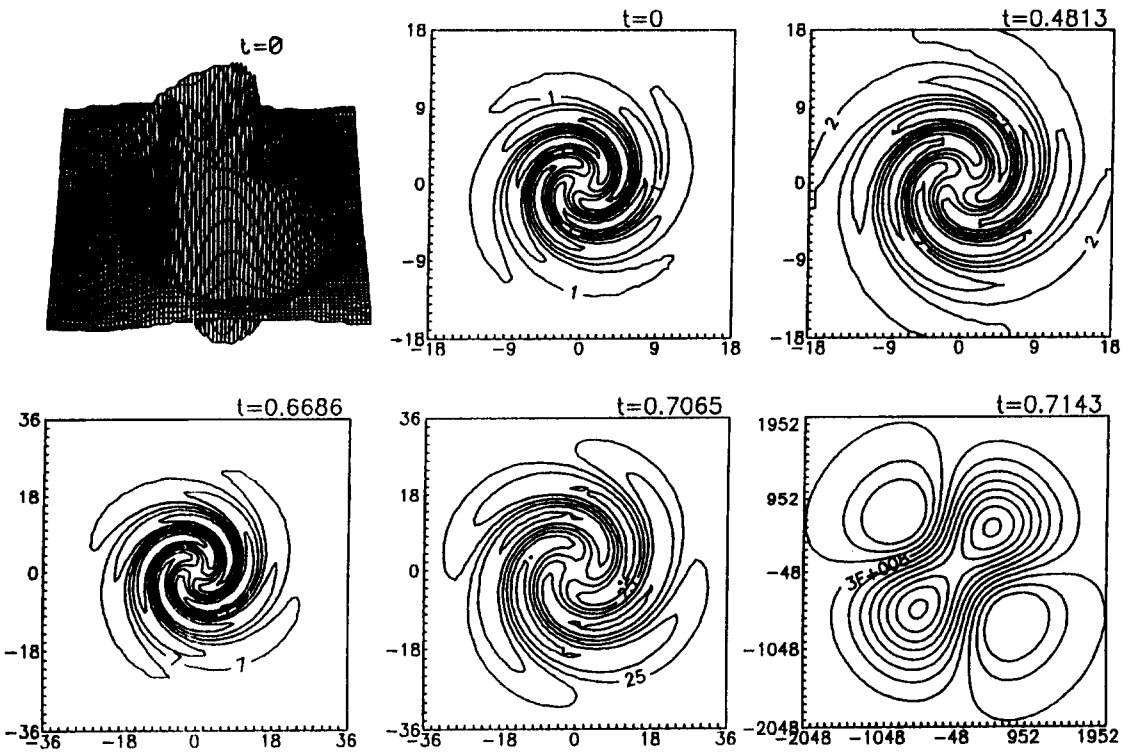

Fig. 4. Evolution of a two-armed spiral wave: $C_0 = 1$, $k = 2$.

equation (7), the blow-up time $\tilde{T}_0$, found when solving the parabolic problem, should be close to T_0. All the examples below confirm this.

The evolution in time of five different eigenfunctions, corresponding to parameters $\sigma = 2$ and $\beta = 2.4$ is shown and analysed. The first two of them determine complex symmetry waves ($C_0 = 0$), the last three-spiral waves ($C_0 = 1$). The exact blow-up time is $T_0 = 1/(\beta - 1) = 0.(714285)$.

Example 1. Fig. 1 ($t = 0$) shows the surface and the level-lines of the eigenfunction with one maximum, one minimum and one axis of symmetry, computed by using the initial approximation (22), (18) with $k = 1$, $\alpha = 1$. In Fig. 1, the level-lines of the solution of the parabolic problem for four different times $t > 0$ are also shown. The blow-up time, found in calculations, is $\tilde{T}_0 = 0.714475$. The values of the maximum ($u_{\max}$) of the solution u, the rescaled errors $e(t)$ defined by (38) and the ratio $t/\tilde{T}_0\%$ are shown in Table 1 for different times t. For $0 \leqslant t \leqslant 0.7108 = 99.49\%\tilde{T}_0$ (see Fig. 1e) the evolution of the maximum follows the self-similar law

$$r(t) = r(0)(1 - t/T_0)^m \approx r(0)\Gamma(t)^{(\sigma+1-\beta)/2},$$

where $\Gamma(t)$ is given in (12).

On the asymptotic stage the background of the solution is dying down in comparison with the core and the complex wave degenerates into a radially symmetric one. The self-similar representation $\Theta(t, \xi, \phi)$ (12) of u tends to the radially symmetric eigenfunction with a finite support for the same

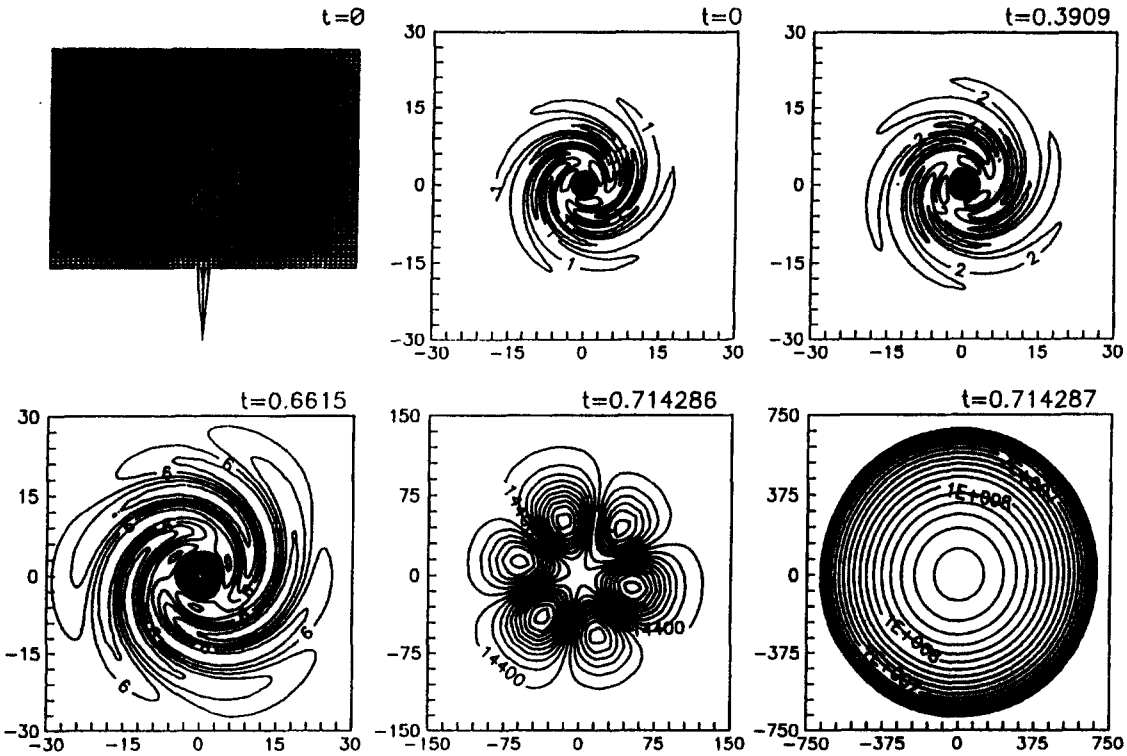

Fig. 5. Evolution of a three-armed spiral wave: $C_0 = 1$, $k = 3$.

Table 1
Metastability of the wave from Example 1

t	$u_{\max}$	$e(t)$	$t/\tilde{T}_0\%$
0.0000	1.175	0.0000	0.00
0.2541	1.614	0.0127	35.84
0.6122	4.786	0.0254	85.69
0.6979	18.314	0.0626	97.68
0.7108	57.126	0.1355	99.49

Table 2
Metastability of the wave from Example 2

t	$u_{\max}$	$e(t)$	$t/\tilde{T}_0\%$
0.0000	1.317	0.0000	0.00
0.5567	3.898	0.0102	77.97
0.6948	17.793	0.0427	97.31
0.7090	47.782	0.1228	99.26
0.7132	189.726	0.4339	99.88

Table 3
Coordinates of the extreme points of a one-armed spiral

t	u_{max}	r_{max}	φ_{max}	ξ_{max}	ϕ_{max}	ξ_{min}	ϕ_{min}
0.0000	1.000097	1.50	3.33	1.50	3.33	1.50	0.19
0.2928	1.458	1.75	3.73	1.56	3.35	1.56	0.21
0.4657	2.126	2.00	4.12	1.60	3.37	1.60	0.23
0.6475	5.433	2.50	5.10	1.50	3.40	1.65	0.27
0.7106	43.021	5.00	0.98	1.62	3.51	1.62	0.36
0.7114	51.878	12.50	3.14	3.82	5.48	3.82	2.34

parameters σ and β. Let us note however that this happens for $t > 99.49\%\tilde{T}_0$: thus, the complex wave, corresponding to this eigenfunction, is metastable.

Example 2. The evolution in time of a complex wave with one maximum, two minima and two axes of symmetry ($k=2$, $\alpha=1$ in the initial approximation (22), (18)) is shown in Fig. 2. The computed blow-up time $\tilde{T}_0 = 0.714287$ is much closer to the exact one. As it is seen from Table 2, this wave is also metastable. On the asymptotic stage the wave degenerates into the same radially symmetric one as in Example 1.

Example 3. The evolution in time of three spiral waves — one-armed ($k=1$, $\alpha=0.05$), two-armed ($k=2$, $\alpha=0.001$) and three-armed ($k=3$, $\alpha=0.001$) — is shown in Fig. 3, Fig. 4 and Fig. 5 respectively.

For the one-armed spiral wave (Fig. 3) the computed blow-up time is again $\tilde{T}_0 = 0.714287$ (see Example 2.). Table 3 contains the maximum u_{max} of the solution u; the coordinates (r_{max}, φ_{max}) of this maximum; the coordinates (ξ_{max}, ϕ_{max}) and (ξ_{min}, ϕ_{min}) of the maximum and the minimum of the self-similar representation $\Theta(t, \xi, \phi)$ (12) for different times t. It shows that for $t \leqslant 0.7106 = 99.48\%\tilde{T}_0$ the maximum and the minimum follow the self-similar law

$$r(t) = r(0)\Gamma(t)^{(\sigma+1-\beta)/2}, \qquad \varphi(t) = \varphi(0) + C_0 \ln \Gamma(t). \tag{39}$$

The eigenfunction is computed on a mesh with step sizes $\Delta\xi = 0.25$, $\Delta\phi = \pi/16 \approx 0.19$.

For the two-armed spiral wave (Fig. 4) $\tilde{T}_0 = 0.71428579$ is much closer to T_0. The evolution of the maximum and the minimum follows the self-similar law (39) up to $t = 0.7065 = 98.91\%\tilde{T}_0$. Degenerating on the asymptotic stage, the wave turns into a wave of complex symmetry (Fig. 4, $t = 0.7143$) before degenerating into the radially symmetric one.

For the three-armed spiral wave (Fig. 5) $\tilde{T}_0 = 0.71428572$. The positions of the two local maxima and the corresponding self-similar trajectories are shown in Fig. 6. Up to time $t = 0.7059$ the positions of the local maxima are the nearest mesh points to the trajectories. After $t = 0.7059 = 98.83\%\tilde{T}_0$ one of the maxima leaves the self-similar trajectory and goes straightforward from the origin, which is typical for waves with complex symmetry. The second maximum follows the self-similar trajectory up to $t = 0.7129$ and after that it dies off. Similarly to the two-armed spiral wave, this one turns into a wave of complex symmetry (Fig. 5, $t = 0.714286$) before degenerating into the radially symmetric one (Fig. 5, $t = 0.714287$).

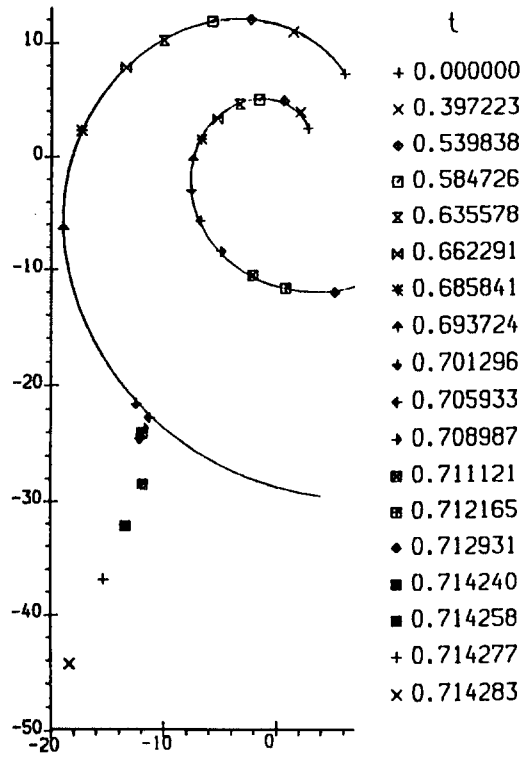

Fig. 6. Motion of the maxima of a three-armed spiral wave.

7. Conclusions and comments

The idea of extending the definition of eigenfunctions of the nonlinear medium by admitting a boundedness instead of vanishing at infinity turned out to be essential for finding blow-up spiral self-similar solutions — a problem which has been open since 1985. Let us note that formation of spiral waves is observed in many chemical, mechanical and biological systems. Convincing examples are the Belousov–Zhabotinskii reaction, the growth of crystals in a rotating magnetic field, spiral shaped convection regimes in Rayleigh–Bénard systems, the organization in cell colonies of social amoebae, the spreading depression in the retina, the exitation waves in the cardiac muscle. During the last 25 years the existence and the behaviour of spiral wave solutions of the mathematical models of such systems have been studied by many specialists (see [1] and the references cited therein). Most of the mathematical models are reaction–diffusion systems of equations (as $\lambda - \omega$ systems) or complex coefficients equations (as Kuramoto–Tsuzuki equation and Ginsburg–Landau equation) with linear diffusion and nonlinear feedback. Probably the nonlinear diffusion in Eq. (2) coupled with the nonlinear feedback is the reason one real coefficients equation to admit spiral wave solutions. Let us note, all mentioned above spiral waves evolve on a nonzero background.

The numerical techniques developed here make it possible to compute waves with complex symmetry as well as spiral ones. Both kinds of waves are metastable — they preserve their structure up to times very close to the time T_0 of their life. Near that time they degenerate into the

simplest radially symmetric blow-up wave, which is the attractor of the wave-processes in this medium.

Thus, the set of possible dissipative structures and waves in the nonlinear medium, described by Eq. (1), is enlarged. Some natural questions arise in this context.

1. How many different complex symmetry waves ($C_0 = 0$) and spiral waves ($C_0 \neq 0$) exist for given parameters $\beta < \sigma + 1$?
2. Do there exist spiral structures for $\beta > \sigma + 1$?
3. Are there structures and waves of some other types of symmetry?

Answers to these questions can not be found by numerical experiments only. Thorough theoretical investigations must be carried out on the multiplicity of the solutions of the nonlinear elliptic equation (7) with boundary conditions (8), (9), or (8), (10), or possibly some others. There are theoretical results concerning the number of the different solutions for the radially symmetric analogue of equation (7) only [19].

Thus some interesting and challenging questions still remain open. The worked-out numerical techniques will hopefully be useful for verification of hypothesis concerning these topics.

Acknowledgements

The authors are very grateful to Dr. V.A. Dorodnicin and Dr. S.R. Svirshchevskii, who posed the problem for finding the spiral eigenfunctions, and to Prof. S.P. Kurdyumov for the helpful discussions.

The work of the first and the fourth authors is supported under Grant MM-425/94 by the Ministry of Education and Science, Bulgaria.

The work of the second and the third authors is supported under Grant MM-501/95 by the Ministry of Education and Science, Bulgaria.

References

[1] T.S. Ahromeeva, S.P. Kurdyumov, G.G. Malinetskii, A.A. Samarskii, Nonstationary Structures and Diffusion-induced Chaos, Nauka, Moscow, 1992 (in Russian).

[2] M.I. Bakirova, S.N. Dimova, V.A. Dorodnicin, S.P. Kurdyumov, A.A. Samarskii, S.R. Svirshchevskii, Invariant solutions of the heat conduction equation describing directed propagation of combustion and helical waves in a nonlinear medium, Sov. Phys. Dokl. 33 (1988) 187–189.

[3] J. Beberness, D. Eberly, Mathematical Problems from Combustion Theory, Springer, Berlin, 1989.

[4] C.M. Chen, S. Larsson, N.-Y. Zhang, Error estimates of optimal order for finite element methods with interpolated coefficients for the nonlinear heat equation, IMA J. Numer. Anal. 9 (1989) 507–524.

[5] S.N. Dimova, M.S. Kaschiev, M.G. Koleva, D.P. Vasileva, Numerical analysis of nonradially-symmetric structures arising in nonlinear reaction-diffusion processes, in: Yu.Yu. Lobanov, E.P. Zhidkov (Eds.), Programming and Math. Methods for Solving Physical Problems, World Scientific, Singapore, 1994, pp. 251–256.

[6] S.N. Dimova, M.S. Kaschiev, M.G. Koleva, D.P. Vasileva, Numerical analysis of radially nonsymmetric structures in nonlinear heat transfer medium, Doklady Russian Acad. Sci. 338 (1994) 461–464 (in Russian).

[7] S.N. Dimova, M.S. Kaschiev, S.P. Kurdyumov, Eigenfunctions for the combustion of a non-linear medium in the radial-symmetric case, USSR Comput. Maths. Math. Phys. 29 (1989) 61–73.

[8] S.N. Dimova, D.P. Vasileva, Numerical realization of blow-up spiral wave solutions of a nonlinear heat-transfer equation, Int. J. Num. Meth. Heat Fluid Flow 4 (1994) 497–511.

[9] S.N. Dimova, D.P. Vasileva, Lumped-mass finite-element method with interpolation of the nonlinear coefficients for a quasilinear heat transfer equation, Numerical Heat Transfer Part B 28 (1995) 199–215.
[10] G.G. Elenin, S.P. Kurdyumov, A.A. Samarskii, Nonstationary dissipative structures in a nonlinear heat-conducting medium, Zh. Vychisl. Mat. Fiz. 23 (1983) 380–390 (in Russian).
[11] V.A. Galaktionov, V.A. Dorodnicin, G.G. Elenin, S.P. Kurdyumov, A.A. Samarskii, The quasilinear heat conduction equation with a source: enhancement, localization, symmetry, exact solutions, asymptotic forms and structure, J. Sov. Math. (JOSMAR) 41 (1988) 1163–1356.
[12] M.K. Gavurin, Nonlinear functional equations and continuous analogues of iterative methods, Izv. Vuz. Matem. 5 (1958) 18–31 (in Russian).
[13] M.G. Koleva, S.N. Dimova, M.S. Kaschiev, Analysis of the eigen functions of combustion of a nonlinear medium in polar coordinates by FEM, Math. Modeling 3 (1992) 76–83 (in Russian).
[14] S.P. Kurdyumov, Evolution and self-organization laws in complex systems, Int. J. Modern Phys. C 1 (1990) 299–327.
[15] S.P. Kurdyumov, E.S. Kurkina, A.B. Potapov, A.A. Samarskii, Complex multidimensional structures of combustion of a nonlinear medium, Dokl. Acad. Nauk SSSR 274 (1984) 1071–1075 (in Russian).
[16] M.-N. Le Roux, H. Wilhelmsson, Simultaneous diffusion, reaction and radiative loss processes in plasmas: numerical analysis with application to the dynamics of fusion reactor plasma, Physica Scripta 45 (1992) 188–192.
[17] H.A. Levine, The role of critical exponents in blowup theorems, SIAM Rev. 32 (1990) 262–288.
[18] V.A. Novikov, E.A. Novikov, Stability control of explicit onestep methods for integration of ordinary differencial equations, Dokl. Akad. Nauk SSSR 272 (1984) 1058–1062 (in Russian).
[19] A.A. Samarskii, V.A. Galaktionov, S.P. Kurdyumov, A.P. Mikhailov, Blow-up in Quasilinear Parabolic Equations, Walter de Gruyter, Berlin, New York, 1995.
[20] A.A. Samarskii, N.V. Zmitrenko, S.P. Kurdyumov, A.P. Mikhailov, Nonlinear effects in plasma, in: Technology of Inertial Confinement Experiments, Technical Document IAEA -200, Vienna, 1977, pp. 185–202.
[21] V. Thomee, Galerkin Finite Elements Methods for Parabolic Equations, Lect. Notes Math., vol. 1054, Springer, Berlin, 1984.
[22] B.A. Trubnikov, S.K. Zhdanov, Unstable quasi-gaseous media, Phys. Rep. 155 (1987) 137–230.
[23] H. Wilhelmsson, Diffusion, creation and decay processes in plasma dynamics: evolution towards equilibria and the role of bifurcated states, Nucl. Phys. A 518 (1990) 89–98.
[24] N.V. Zmitrenko, S.P. Kurdyumov, A.P. Mikhailov, A.A. Samarskii, Localization of thermo-nuclear combustion in plazma with electronic heat conductivity, Lett. JETPh 26 (1977) 620–624 (in Russian).